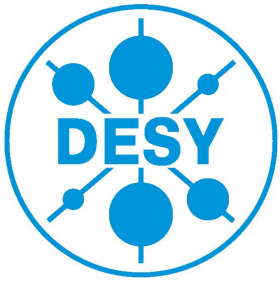

Saturation in high energy *pp* interactions at the LHC

Khilesh Mistry

University of California Santa Cruz, California, U.S.A.

Summer 2012

Supervisors: Hannes Jung, Panos Katsas, Albert Knutsson

Abstact

We studied the saturation and multi-parton effects in high energy interactions at the LHC. We made use of the PYTHIA and CASCADE Monte Carlo generators to study the effects of charged hadron distributions in the low momentum fraction regime where saturation in parton distribution functions is supposed to become prevalent. We found that the inclusion of saturation is not necessary to describe the charged hadron distribution, but the low $p_\perp$ region needs to be further studied as there are many puzzling and interesting results.

Contents

1 Introduction

At the current time, the Large Hadron Collider (LHC) at CERN (Organisation europenne pour la recherche nuclaire) is the world's largest and most powerful particle accelerator [Fig. 1]. The LHC has four main experiments, with the goal of deepening our understanding of the standard model of particle physics as well as looking to find physics beyond the standard model. Some of the fundamental questions driving the project are : Is the Higgs mechanism of mass generation and spontaneous electroweak symmetry breaking correct? Is there supersymmetry in nature? What is dark matter?

The LHC is located on the Switzerland-France border near Geneva and is buried over 150 meters deep, residing in a tunnel of 27 km in circumference. It was designed collide protons at an energy of $\sqrt{s} = 14$ TeV (center of mass energy). Right now it is running at $\sqrt{s} = 8$ TeV. At the end of 2012 is will be shut down for upgrades and will start up again in 2014 at $\sqrt{s} = 14$ TeV. The multipurpose detectors are the Compact Muon Solenoid (CMS) and A Toroidal LHC ApparatuS (ATLAS), both of which are capable of astonishingly precise measurements. The other two are the Large Hadron Collider beauty (LHCb), built to measure CP violation parameters in b-hadrons and A Large Ion Collider Experiment (ALICE), built to better understand properties of quark-gluon plasma through lead ion (Pb-Pb) collisions.

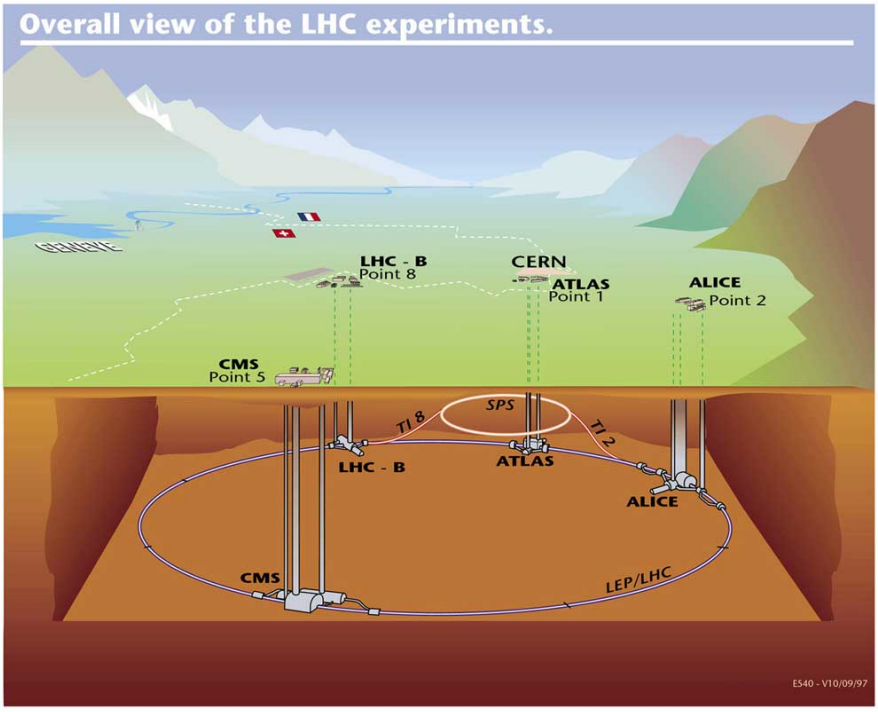

Figure 1: The LHC and experiments

2 The Compact Muon Solenoid Detector

The analysis in this project was done using data from the Compact Muon Solenoid (CMS) detector. There are over 3,600 people from 183 scientific institutions in 83 nations who built the detector, maintain the detector, and analyze the data from the detector.

CMS has a size of 21.5x15x15 meters (l,w,h) and is the heaviest detector in the world, weighing in at 12,500 tons [Fig. 2]. It is broken up in to 5 main layers, shown in [Fig. 3] [4]. After the interaction point, the immediate surrounding area is the tracker which consists of 13 layers (14 at endcaps) and 9.6 million silicon strip channels. The first three layers have pixel arrays; 66 million 100x50 μm silicon pixels. The remaining layers have silicon strip detectors of varying size. In total the tracker has 205 meters squared of silicon sensors [4].

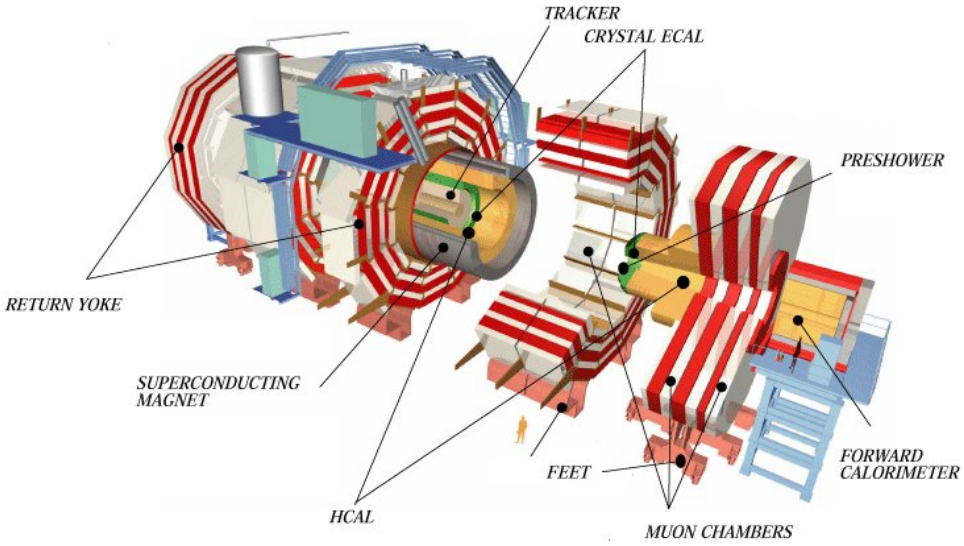

Figure 2: The CMS detector

After the tracker comes the Electromagnetic Calorimeter (ECAL), designed to measure the energy deposition of electromagnetically interacting particles, such as the photon and electron, with unprecedented accuracy. The ECAL consists of lead tungstate ($PbWO_4$), which is a dense, clear material. Each crystal, 22x22x230 mm, is attached to a silicon avalanche photodiodes for readout. There are 61,200 crystals in the barrel of CMS and 7,324 in each endcap [4].

The next layer is the Hadronic Calorimeter or HCAL. Its purpose is very similar to the ECAL, but instead of measuring photons and electrons, it measures the energy of

individual hadrons produced in interactions. The HCAL is made up of layers of brass and steel, interleaved between scintillators and readout by hybrid photodiodes.

Next is where CMS gets its name from; the solenoid magnet. The solenoid magnet of CMS is 13 meters long and 6 meters in diameter. The magnet was designed to run at 4.0 Tesla, but runs at only 3.8 Tesla to increase the lifetime of the detector [4]. The purpose of the magnet is to deflect charged particles so their paths become curved. This provides a way to determine the charge/mass ratio of the particle.

The last layer of the detector is the muon detectors and magnet return yoke. CMS employs 3 techniques to detect muons; Drift Tubes (DT), Cathode Strip Chambers (CSC) and Resistive Plate Chambers (RPC) which are separated into 4 layers and interleaved with the magnet return yoke [4]. DTs are used exclusively in the barrel region and CSC are used only in the endcaps. The RPCs are used both the endcaps and in the barrel and provide fast signals.

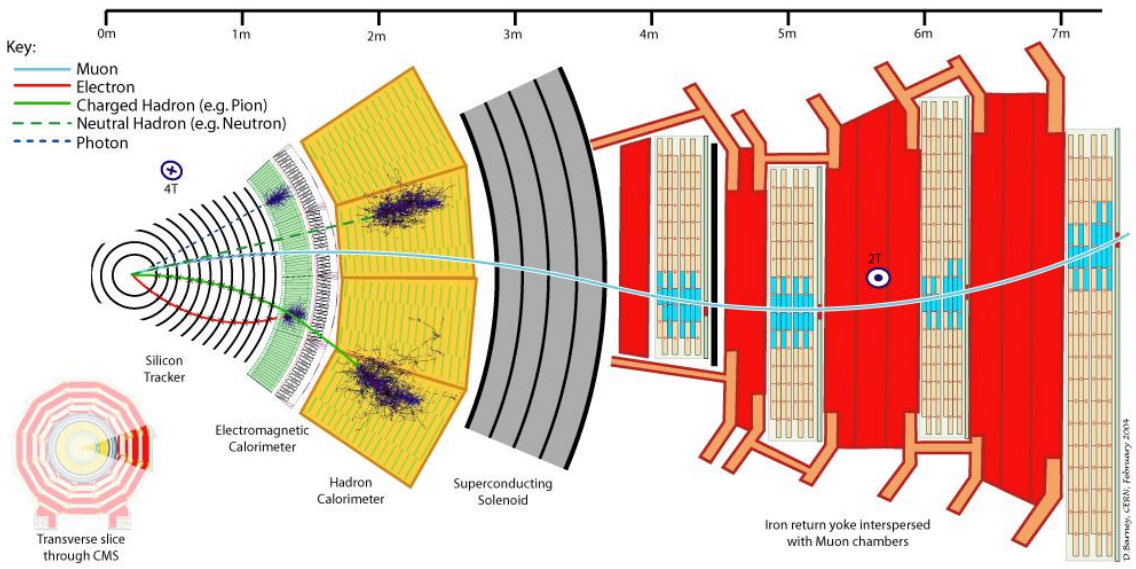

Figure 3: A cross-sectional view of the CMS detector

3 Motivation and Theory

Quantum Chromodynamics is the theory of the strong interaction. It is one of the fundamental parts of the standard model of particle physics and is described by a non-ablelian gauge theory, namely the $SU(3)$ Yang-Mills theory of color-charged fermions. QCD is the dominant process in today's high energy accelerators such as the LHC.

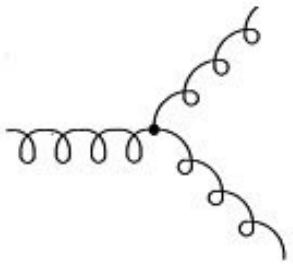

Figure 4: A triple gluon vertex

QCD has its roots inherently in nuclear physics and trying to understand how protons and neutrons interact. It was realized that there were constituents to the proton and soon after, quarks were discovered. Six quarks are the main constituents of hadronic matter, with gluons acting as the "glue" holding the quarks together. The gluons are the generators of the $SU(3)$ color group and an interesting behavior of gluon self interaction [Fig. 4] was predicted due to the non-ablelian nature of the the theory. This is very different from Quantum Electrodynamics as the photon does not self-interact, deriving from the ablelian nature of the theory. Other notable properties of QCD include quark confinement, meaning the force between quarks does not weaken as they are drawn apart; and asymptotic freedom, in very high energy interactions quarks and gluons interact very weakly.

Deep Inelastic Scattering (DIS) of electrons on a proton target is one of the ways to probe the structure of the proton. A diagram of a typical DIS collision can be seen in [Fig. 5]. Parton Distribution Functions (PDFs), the probability density to find a parton (quark or gluon) carrying a momentum fraction (x, $\frac{p_{parton}}{p_{proton}}$) at a certain energy, were measured through the later part of the twentieth century, and were measured very precisely at HERA (DESY). These measurements were a huge triumph for the Quark-Parton Model (QPM) in which the proton is seen as a composition of quarks and gluons (partons).

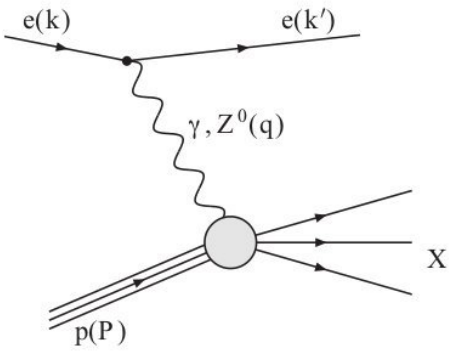

Figure 5: Scattering of an electron off a parton in DIS

In low energy collisions of protons, valence quarks are the main interacting partons. As the energy increases partons radiate other partons with probability [6]

$$\alpha_s \int \frac{1}{x} dx \sim \alpha_s ln(\frac{1}{x}) \tag{1}$$

At small parton densities the parton density evolution is described by 3 equations; the BFKL (Balitsky-Fadin-Kuraev-Lipatov) and CCFM (Catani-Ciafaloni-Fiorani- Marchesini) at low momentum fraction (x), and the DGLAP (Dokshitzer-Gribov-Lipatov-Alterelli-Parisi) at higher momentum transfer (Q^2) and fraction (x). A graphical description of this can been seen in [Fig. 16]. Over several orders of magnitude, the DGLAP equation agrees with measurement incredibly well. The DGLAP equation for gluons and quarks in leading order of α_s can be seen below [6]. For quarks (inlcuding the gluon part)

$$\frac{dq_i(x,\mu^2)}{d\log\mu^2} = \frac{\alpha_s}{2\pi}\int_x^1 \frac{d\xi}{\xi}\left[q_i(\xi,\mu^2)P_{qq}\left(\frac{x}{\xi}\right) + g(\xi,\mu^2)P_{qg}\left(\frac{x}{\xi}\right)\right] dx \tag{2}$$

and for gluons

$$\frac{dg(x,\mu^2)}{d\log\mu^2} = \frac{\alpha_s}{2\pi}\int_x^1 \frac{d\xi}{\xi}\left[\sum_i q_i(\xi,\mu^2)P_{qg}\left(\frac{x}{\xi}\right) + g(\xi,\mu^2)P_{gg}\left(\frac{x}{\xi}\right)\right] dx \tag{3}$$

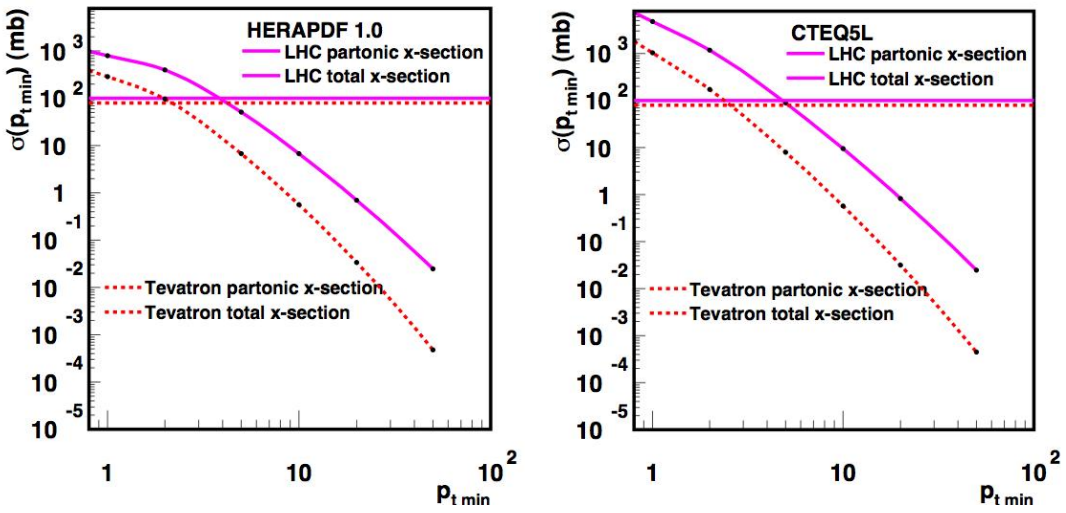

Figure 6: Partonic cross sectional measurements at the LHC and Tevatron

At low momentum fraction, partons overlap in phase space and parton recombination begins. Thus we have a problem: the DGLAP equation does not work for low x and the BFKL equation predicts a fast rise in gluon density. The model predicts a partonic cross section that rises faster than $\frac{1}{p_{\perp min^2}}$ as $p_{\perp min}$ goes to zero, leading to a partonic cross section which exceeds the total inelastic (non-diffractive) cross section. In Figure 6 there are plots of two different PDF sets from the LHC and the Tevatron showing this divergent cross section. This unitary violation leads to the idea of multi-parton interactions [6]. In Fig. 7 on the left you can see the standard $2 \rightarrow 2$ process (2 partons interacting to produce a final state of a 2 quarks - a $q\bar{q}$ pair) for a proton-proton colli-

sion. On the right you can see the multi-parton approach, in which the main interaction happens between two sets of partons rather than only one.

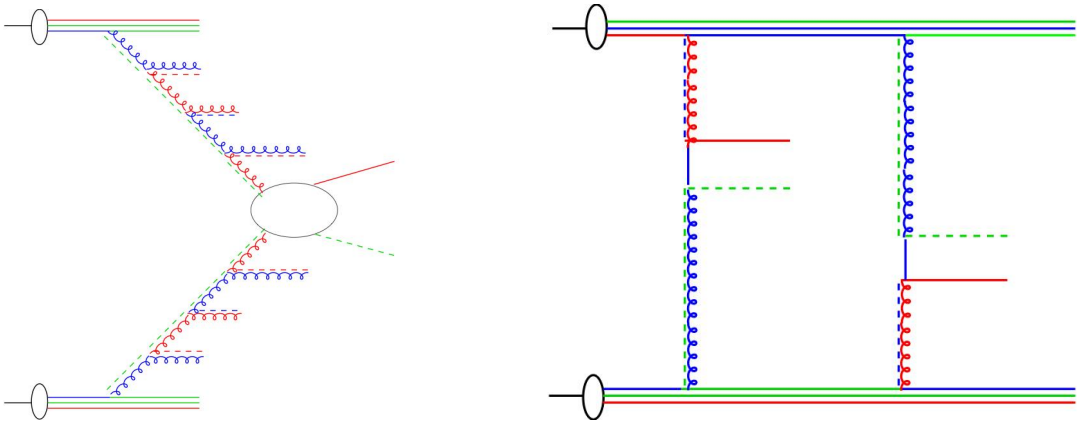

Figure 7: Left - Standard 2→2 process **Right** - with MPI

Multi-parton interactions (mentioned above) and saturation are some of the potential solutions to solving this divergent QCD cross section. Saturation is a an effect at low Q^2 and low momentum fraction in which the gluons interact with each other, recombine, and overlap in such a way that they slow the rise in gluon density. These two concepts were the most important motivation factors in this project. We wanted to study multi-parton interaction (MPI) effects in multiple Monte Carlo generators and study how running the MC generator with different PDFs with and without saturation affected the results.

4 Monte Carlo and Analysis

This project employed the technique of Monte Carlo simulations. Monte Carlo takes advantage of random numbers and sampling for a system of many coupled degrees of freedom. It is especially useful in complicated systems and systems where one can not solve equations for an solution analytically, such as Quantum Chromodynamics. In this project two different Monte Carlo generators were used, PYTHIA and CASCADE, with different parameters and different tunes(different parton interaction settings) to simulate proton-proton collisions at various LHC energies.

For the PYTHIA Generator, an interface known as AGILe (A Generator Interface Library and executable) provided a role of steering interface. This allows for a change in the settings of the generator such as beam energy, MPI effects, PDFs, and number

of events through a simple command line interface. AGILe interfaces FORTRAN-based Monte Carlo generators with C++ HepMC event records. Using this event record one can back track everything which happens in a particular generated event. AGILe pipes the events out into a FIFO (First in, First out file), which is then read in through the front end of a validation tool called RIVET (Robust Independent Validation of Experiment and Theory). RIVET is a tool in which one can write experimental analyses and run current RIVET validated analyses to analyze MC data and check generators for consistency. RIVET's design allows for multiple event generators to interface with it, as long as the HepMC records are read in. In this way, the same analysis could be done on both different generators. After the analysis was done, one could use RIVET or ROOT to make histograms and plots. A graphical description of this process can be seen in [Fig. 8].

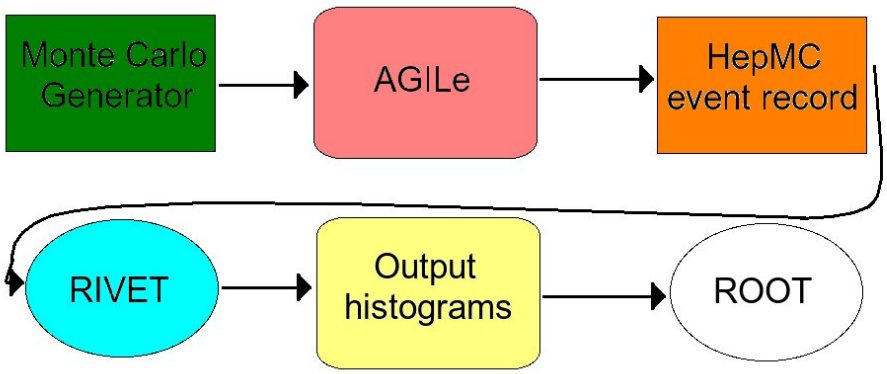

Figure 8: A graphical description of how events are generated to how they are analyzed

The analyses used in this report were RIVET standard analyses written for the CMS collaboration. They are CMS_20 _S8547297 and CMS_2010_S8656010, both written by Albert Knutsson. The data compared with it is from the CMS collaboration and was taken in 2010, titled *Transverse momentum and pseudorapidity distributions of charged hadrons in pp collisions at sqrt(s) = 0.9 and 2.36TeV (Khachatryan 2010)* and *Transverse momentum and pseudorapidity distributions of charged hadrons in pp collisions at sqrt(s) = 7TeV (Khachatryan 2010)* [1] [2]. A study of charge hadrons distribution as a function of $p_\perp$ (transverse momentum) and η was looked at to see any MPI or saturation effects.

5 Results and Discussion

5.1 PYTHIA6

To look at saturation and MPI effects, an approach similar to that of Eugene Levin was followed. Looking at charged hadron distributions in transverse momentum ($p_\perp$), one can extract different information about multi-parton effects and saturation [3].

One of the first studies carried out was the study of MPI effects and the PYTHIA 'taming' parameter. This 'taming' parameter is a phenomenological addition to the PYTHIA generator in order to tame the divergent partonic cross section (mentioned in Motivation and Theory [Fig. 6]).The 'taming' parameter is added onto matrix elements and is the last part of the equation below.

$$\|M\| \sim \frac{\alpha_s}{t^2} \sim \frac{\alpha_s}{{p_\perp}^2} \sim \frac{\alpha_s({p_\perp}^2 + p_{\perp 0}^2)}{\alpha_s({p_\perp}^2)} * \frac{{p_\perp}^4}{({p_\perp}^2 + p_{\perp 0}^2)^2} \tag{4}$$

In this study the 'taming' parameter was first removed by setting $p_{\perp 0}$ to zero, making the last term equal to 1. In Figure 9 one can see that the PYTHIA MC does not match the data well at all with the 'taming' parameter neutralized and multi-parton interactions turned off. In the next figure, with MPI still off and the 'taming' parameter turned on, there is a considerable change to the spectra [Fig. 10] (blue). This change brings the MC closer to the data but still is not in good agreement. Figure 10 (green) shows the PYTHIA simulation with this 'taming' parameter and MPI on. There is superb agreement between data and PYTHIA in this case.

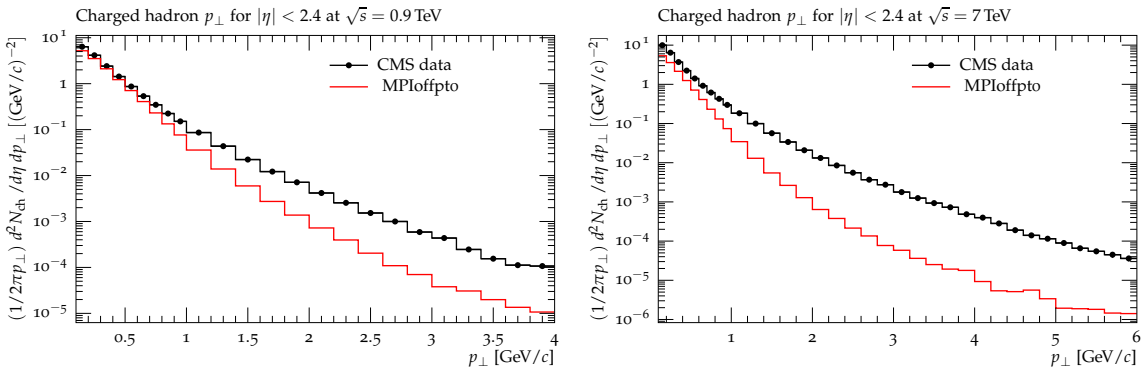

Figure 9: Charged hadron distribution of data and PYTHIA MC generator with MPI off and 'taming' parameter turned off($\sqrt{s} = 900$GeV on left, $\sqrt{s} = 7$TeV on right).On the x-axis is the $p_\perp$ and on the y-axis is the average number of charged particles per event within $\|\eta\| < 2.4$ data of this plot and all charged hadron distributions from the CMS collaboration [1] [2]

Looking at not only the $p_\perp$ distributions, but in also the integrated η distributions, one can also learn quite a bit about what is happening at small $p_\perp$. In Figure 11 one can see the opposiste effect: the MPI is the dominant part, rather than the 'taming' of

the cross section. This is not telling us contradictory information, but just that MPI plays a bigger part in lower $p_\perp$ bins.

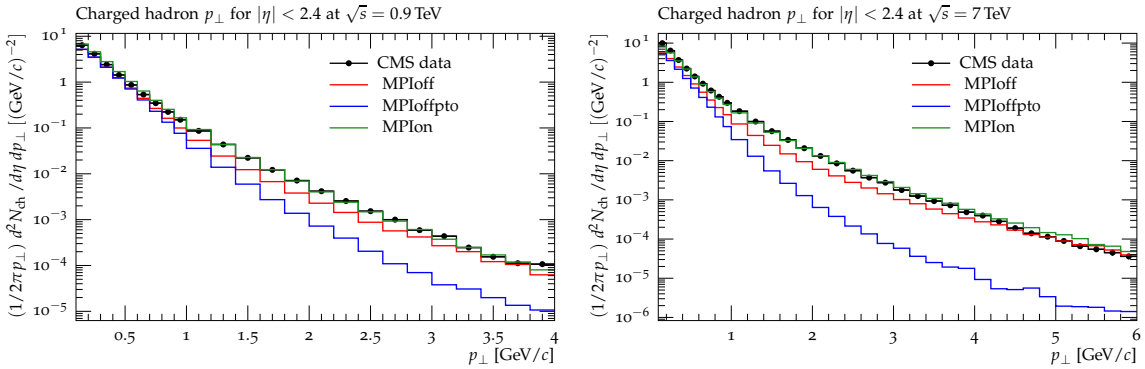

Figure 10: Charged hadron distribution of data and PYTHIA MC generator with 'taming' parameter on ($\sqrt{s} = 900$GeV on left, $\sqrt{s} = 7$TeV on right). Green line corresponds to the simulation with MPI and 'taming' parameter turned on and the blue line corresponds to only the 'taming' parameter turned on

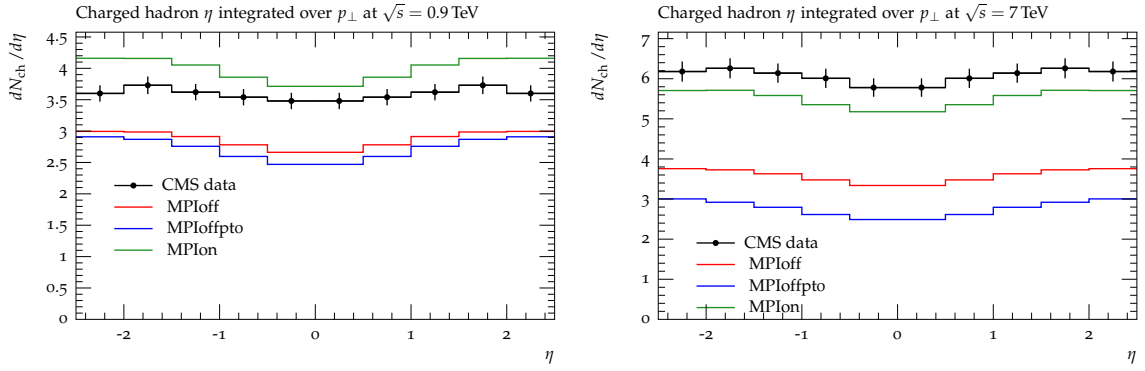

Figure 11: Charged hadron distribution of data and PYTHIA MC generator with 'taming' parameter on ($\sqrt{s} = 900$GeV on left, $\sqrt{s} = 7$TeV on right). Note the main difference is between MPI on/off rather than the 'taming' parameter

Continuing on with understanding the behavior of the 'taming' parameter, the next step was to understand what PYTHIA does internally as it make $p_\perp$ cuts. This was done by adjusting values of the CKIN(3) , the $p_\perp$ cut parameter, and the $p_{\perp 0}$ parameter, the minimum allowed $p_\perp$. Setting $p_{\perp 0}$ to zero again and changing the CKIN(3) value we saw a small rise in the charged hadron distribution spectra. This is due to a lower allowed minimum $p_\perp$ value, but still the 'taming' parameter is the most dominant effect. Plots of this study can be seen in the Appendix [Fig. 17].

The previous studies were done with the default parton distribution function in PYTHIA. We wanted to study the effects of saturated PDFs and see if saturated PDFs are necessary to describe the charged hadron distribution picture. Figure 18 in the

Appendix shows the difference between the PYTHIA default PDF and the saturated one. The saturated PDF exhibits large behavior at small x compared with the non-saturated PDF. This is slightly counter intuitive and is due to the "slower" evolution and the large saturation scale at low $p_\perp$ [3]. With the inclusion of the EHQS PDF in PYTHIA, there was a very small effect on the charged hadron distribution [Fig. 12]. Most of the changes come from MPI and the partonic cross section problem, rather than from this saturation effect.

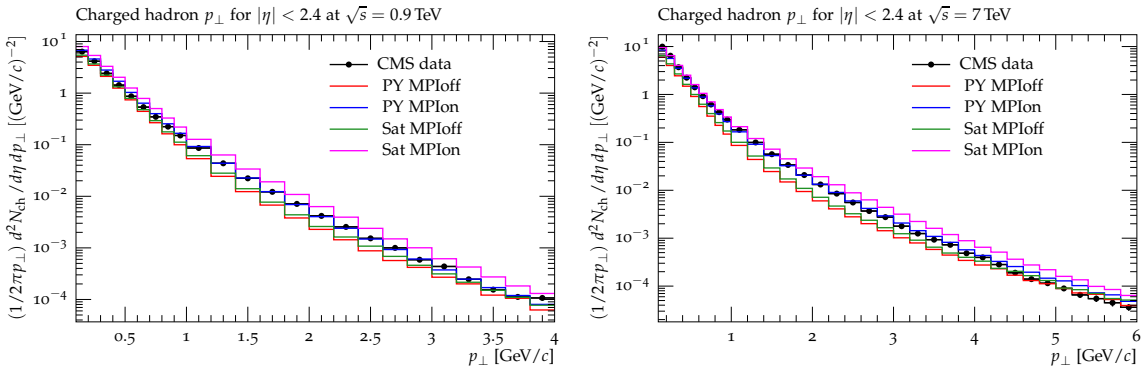

Figure 12: Charged hadron distribution of data and PYTHIA MC generator with the EHKS saturated PDF ($\sqrt{s} = 900$GeV on left, $\sqrt{s} = 7$TeV on right).

The final analysis in PYTHIA that was done was to look at different PYTHIA tunes and see how they handled this saturated PDF and MPI interactions. Different tunes are different parameter sets which describe different ways to handle parton interactions and effects. The comparison of the default PYTHIA, Z2*, and D6T tunes can be seen in [Fig 13]. These different tunes essentially gave the same results even though they treat parton interactions differently. There was also little difference in the saturation effect of these different tunes.

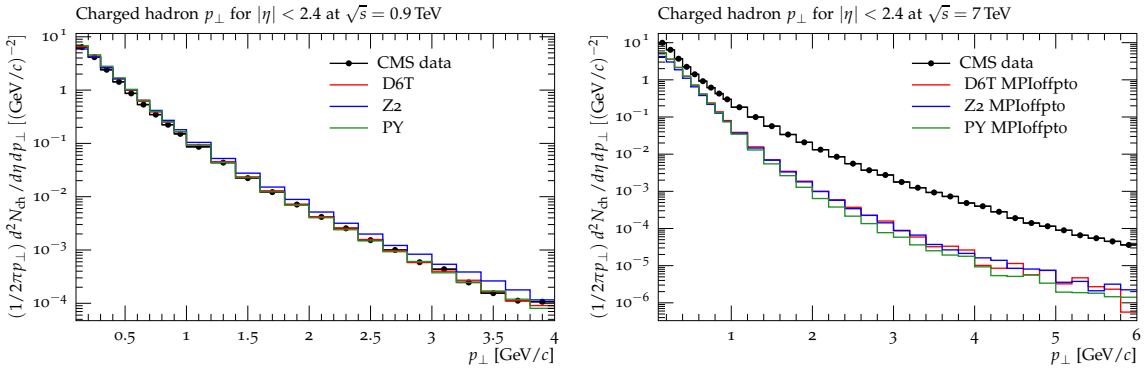

Figure 13: Charged hadron distribution of data and PYTHIA MC with different tunes; default, Z2, D6T($\sqrt{s} = 900$GeV on left, $\sqrt{s} = 7$ TeV on right).

5.2 CASCADE

The CASCADE generator inherently does not have MPI, so comparing these studies straight to PYTHIA and data would be unwise. Instead CASCADE was used to observe purely the *effects* of the PDFs. In CASCADE we tested the GBW (Golec-Biernat-Wustoff) saturated PDF and two unintegrated PDFs (uPDFs). Unintegrated means that instead of the parton distribution function being a function of only μ^2 and x, there is no explicit integral over k_t, making the PDF a function of k_t, μ^2, and x. Thus the uPDF has another degree of freedom. In the Appendix are three PDFs used in CASCADE plotted against each other [Fig. 19].

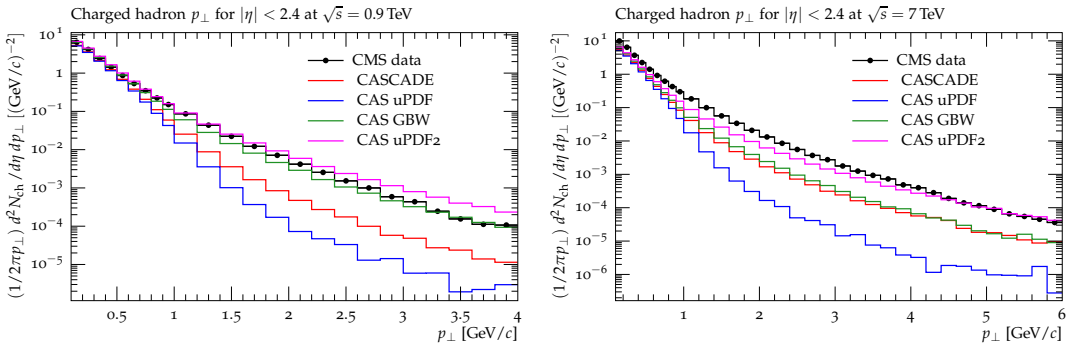

Figure 14: Charged hadron distribution of data and CASCADE generator with different PDFS. Note CASCADE does not have MPI($\sqrt{s} = 900$GeV on left, $\sqrt{s} = 7$TeV on right).

The default settings in CASCADE are with an evolved PDF (red line)[Fig. 14]. This is contrasted with GBW(green), which has no evolution but with a saturated PDF, with uPDF(blue), which was GBW with CCFM evolution, and uPDF2(pink) which is like default CASCADE, but evolved using CCFM with different evolution parameters. From these plots we can learn quite a bit about the nature of the MPI and the saturated GBW PDF.

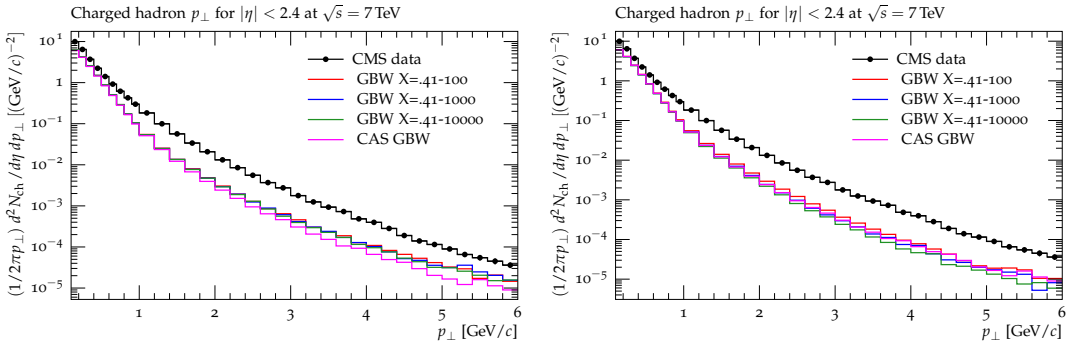

Figure 15: The effects changing the momentum fraction (x) slope of the GBW PDF from 0.1(left) to 0.4(right) The different lines correspond to different onset of saturation variables ($\sqrt{s} = 7$ TeV).

We also tried looking at the saturated GBW PDF in detail. By adjusting the parameters of the small momentum fraction slope of the PDF and changing where saturation began, we thought maybe we could understand some of the behavior slightly better [5]. Unfortunately, changing the slope variable from 0.1 to 0.4 and the onset of saturation by 2 orders of magnitude barely made a difference in the results. These can be seen in [Fig. 15].

6 Conclusions

In conclusion, the 2 $\rightarrow$2 QCD process with parton showering and hadronization can describe the charged hadron spectra. The PYTHIA phenomenological 'taming' parameter actually plays the biggest role in bringing the MC inline with the data. The rest of the difference between MC and the data can be attributed to multi-parton interactions. Though that is in the big picture, but multi-parton interactions play a much larger effect than the taming parameter in the low $p_\perp$ region.

Overall CASCADE helped in learning about the PDFs and saturation effects. Some work still needs to be done to understand why the the unintegrated parton distribution functions act they way they do, why GBW at 900 GeV acts so differently to 7 TeV, and why changing the GBW parameters had such a little effect on the charged hadron distribution? These were all questions that were going to be investigated, but because of time constraints they will have to be done at a later date.

The addition of saturated PDFs does not play a big part in the small $p_\perp$ charged hadron distribitions, and for now are not needed. Though in the future identifying small $p_\perp$ behavior of the QCD cross section will be necessary to solve the problem of the unitarity violation at small $p_\perp$. This may or may not include saturation effects, but will most defintely include multi-parton interactions.

Acknowledgements

First off I would like to thank DESY and all the people at DESY. In particular, I would like to thank Olaf Behnke, Doris Eckstein, Andrea Schrader, and all the summer student organizers. Not only did they assist with logistics and administration of the summer student program, but also with making our stay as pleasurable as possible. I would also like to thank my supervisor, Hannes Jung, whom I have learned quite a bit from. From interesting aspects of high energy physics analysis and histograms to low momentum fraction QCD I really have learned a plethora of new things under his guidance. I would also like to thank my other supervisors here at DESY, Albert Knutson and Panos Katsas as well as everyone in the CMS group I worked in (Mira, Narongrit,Nastja, Nipol, Paolo, Pedro, and Samantha).

I would also like to thank my advisers back at the University of California Santa Cruz, Bruce Schumm and Vitaliy Fadeyev, whose advice and supervision I have been under the past 2 years.

And lastly, I would like to thank my officemate, David Ciupke, for making the work-day slightly less tedious and for distracing me all the time.

References

[1] V. Khachatryan *et al.* [CMS Collaboration], Phys. Rev. Lett. **105** (2010) 022002 [arXiv:1005.3299].

[2] CMS Collaboration, JHEP **1002** (2010) 041 [arXiv:1002.0621].

[3] E. Levin and A. H. Rezaeian, AIP Conf.Proc.1350:243-253,2011 [arXiv:1011.3591].

[4] Della Negra, Petrilli, Herve, Foa, (2006) *CMS Physics Technical Design Report Volume I: Software and Detector Performance* CERN.

[5] K. Golec-Biernat and M. Wustoff, Phys. Rev. **D60:114023** ,1999 [arXiv:9903358]

[6] H. Jung *QCD and Monte Carlo Lectures* writeup (2011)

Appendix

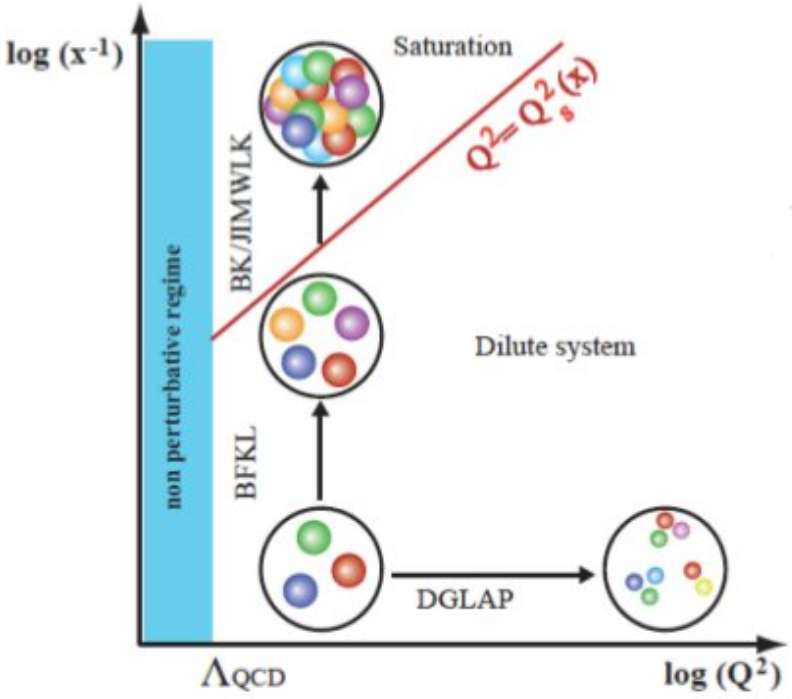

Figure 16: Graphical description of different regimes of the evolution equations

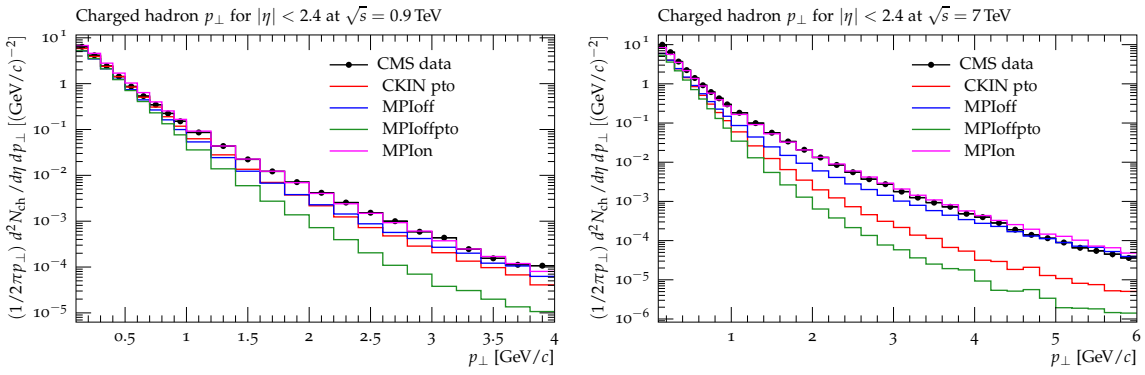

Figure 17: The effects on the charged hadron distribution of studying the CKIN(3) parameter in PYTHIA ($\sqrt{s} = 900$GeV on left, $\sqrt{s} = 7$TeV on right).

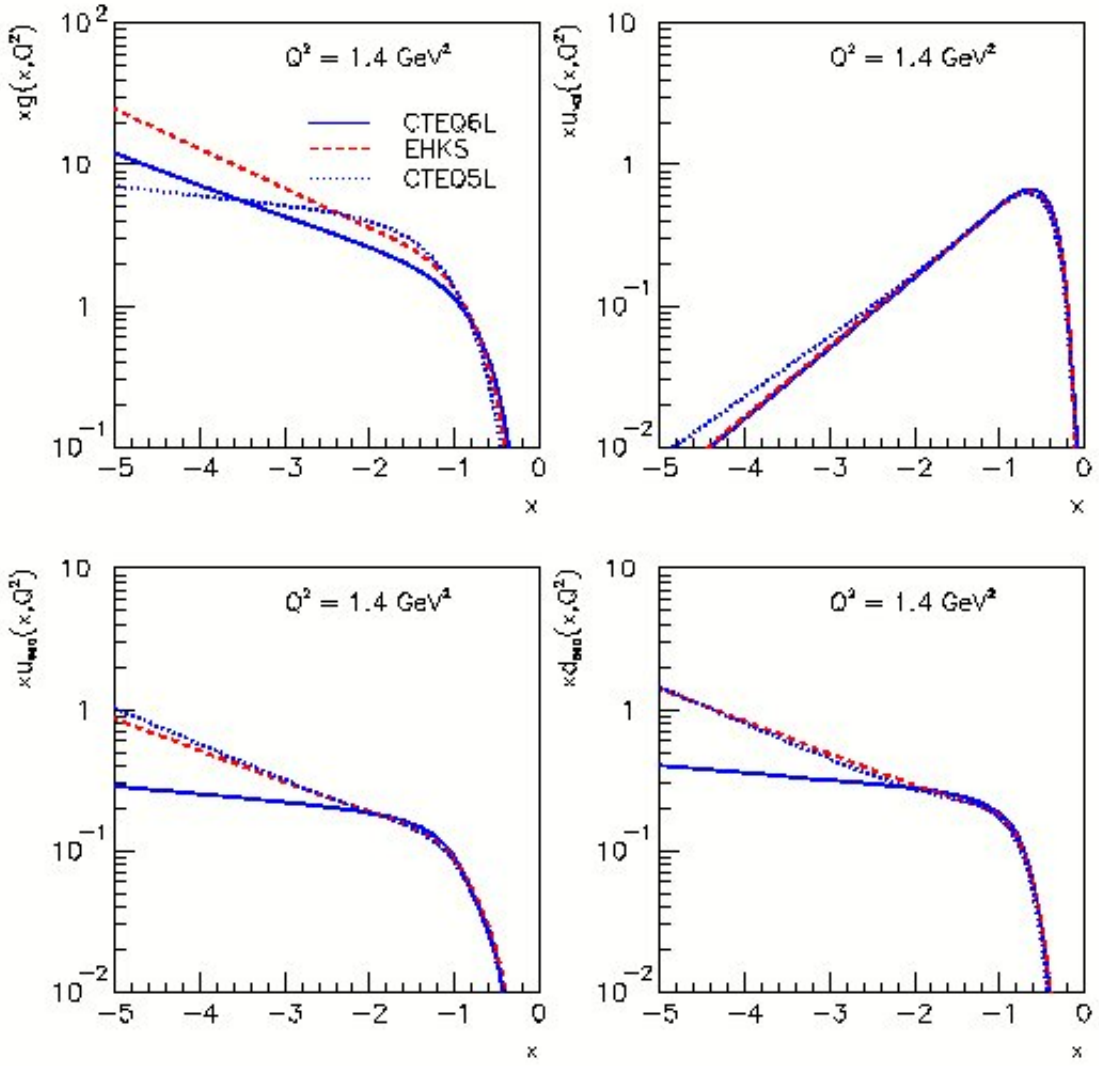

Figure 18: The parton distribution functions used in PYTHIA.CTEQL is what PYTHIA uses as a default. EHKS is the saturated PDF PYTHIA uses.

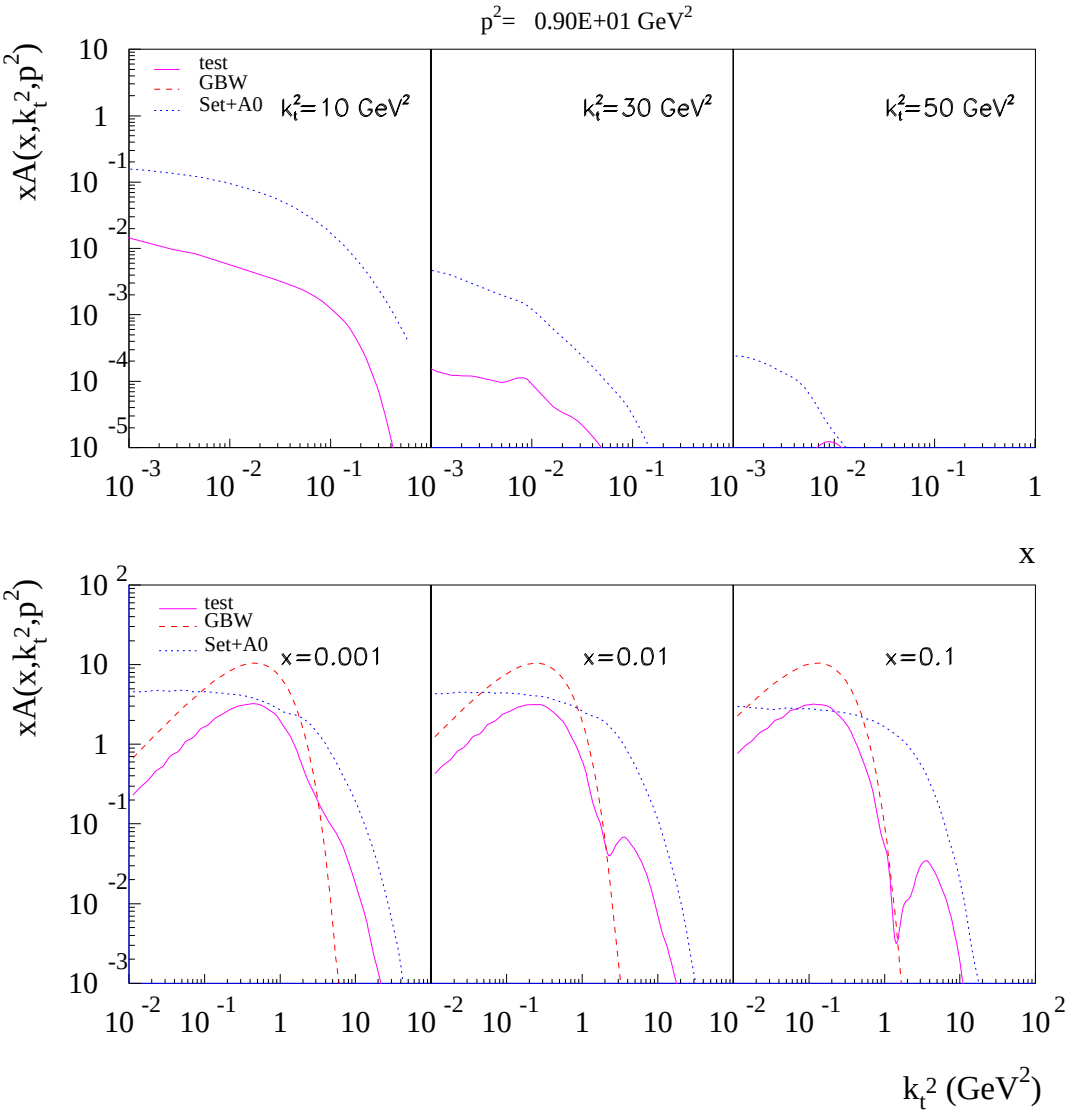

Figure 19: The parton distribution functions used in CASCADE.test is the GBW saturated PDF evolved with CCFM, GBW is regular GBW saturated, and Set+A0 is default CASCADE PDF.